

Jieqing Zheng¹, Xuehao Hu¹, Karima Chah^{1,2} and Christophe Caucheteur^{1,2}

¹Advanced Photonic Sensors Unit, Department of Electromagnetism and Telecommunication, University of Mons, Mons 7000, Belgium

²WEL Research Institute, avenue Pasteur, 6, 1300 Wavre, Belgium

Context Tilted fiber Bragg gratings (TFBGs) exhibit high refractive-index (RI) sensitivity but their broad spectra hinder wavelength-division multiplexing, restricting them to single-point sensing. This work presents a multi-point RI sensing approach using cascaded bare TFBGs interrogated in a single optical channel. By applying first-order derivative spectrum analysis, individual cut-off modes are effectively separated despite strong spectral overlap. A three-point array demonstrates sensitivities of 52.96–57.53 nm/RIU, linearities of $R^2 = 0.94$ –0.98, and mutual interference below 0.03 nm, enabling scalable and cost-effective quasi-distributed RI sensing.

➤ Experimental setup & spectra

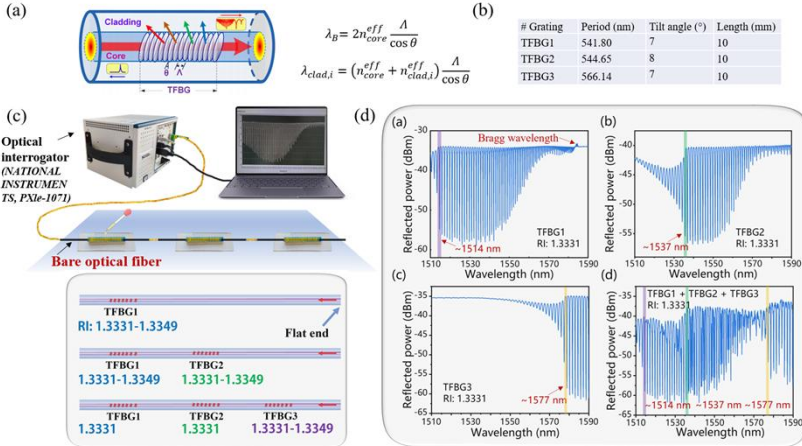


Fig. 1 (a) TFBG sensor structure and principle; (b) main parameters of the 3 TFBGs used in our experiments; (c) schematic diagram of the experimental set-up used to interrogate the cascade of TFBGs and design of experimental sensing schemes; (d) two-pass transmission amplitude spectrum of TFBG1, TFBG2, TFBG3 and the cascade TFB1-TFBG2-TFBG3, each immersed in a 1.3331 RI solution.

➤ Surrounding RI measurements with TFBG1 using derivative method

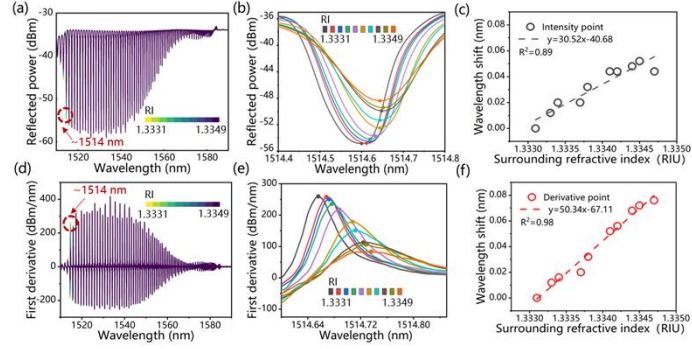


Fig. 2 (a) Evolution of the two-pass transmission amplitude spectrum of TFBG1 as a function of the surrounding RI value; (b) zoomed-in spectrum around the cut-off mode resonance; (c) wavelength of the cut-off mode resonance as a function of the surrounding RI value; (d) evolution of the derivative of the two-pass transmission amplitude spectrum of TFBG1 as a function of the surrounding RI value; (e) zoomed-in derivative of the spectrum on the most sensitive region corresponding to the cut-off mode location; (f) wavelength of the local maximum of the derivative-based demodulation method as a function of the surrounding RI value.

➤ Surrounding RI measurements with TFBG1 and TFBG2 in cascade

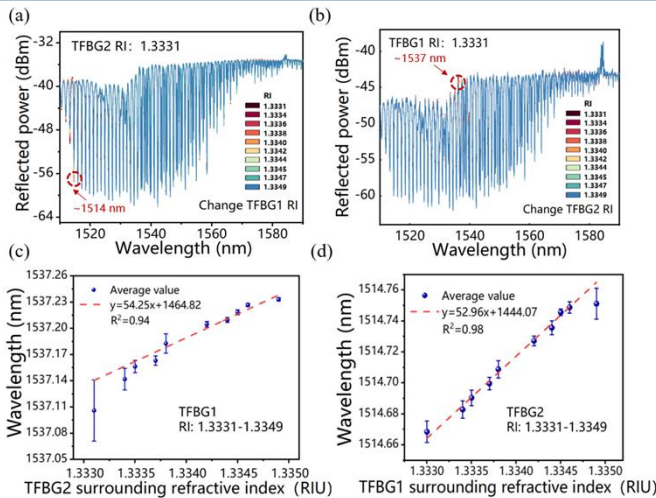


Fig. 3 (a) Evolution of the two-pass transmission amplitude spectrum ~1514 nm of the TFBG1-TFBG2 cascade, as a function of the TFBG1 surrounding RI value (TFBG2 RI: 1.3331); (b) evolution of the two-pass transmission amplitude spectrum ~1537 nm of the TFBG1-TFBG2 cascade, as a function of the TFBG2 surrounding RI value (TFBG1 RI: 1.3331); (c) evolution of derivative spectral peak of TFBG1 around the cut-off ~1514 nm with varying TFBG1 RI between 1.3331-1.3349; (d) evolution of derivative spectral peak of TFBG2 around the cut-off ~1537 nm with varying TFBG2 RI between 1.3331-1.3349.

➤ Comparison of key sensing performance metrics before and after cascading

Sensor configuration	Processing method	Sensitivity (nm/RIU)	Linear correlation (R^2)	Noise level (nm)
Single TFBG1 (independent)	Raw spectrum	30.52	0.89	-
Single TFBG1 (independent)	1st-derivative	50.34	0.98	-
Cascaded TFBG1	1st-derivative	52.96	0.98	0.03
Cascaded TFBG2	1st-derivative	54.25	0.94	0.04
Cascaded TFBG3	1st-derivative	57.53	0.97	-

➤ Surrounding RI measurements with TFBG1, TFBG2 and TFBG3 in cascade

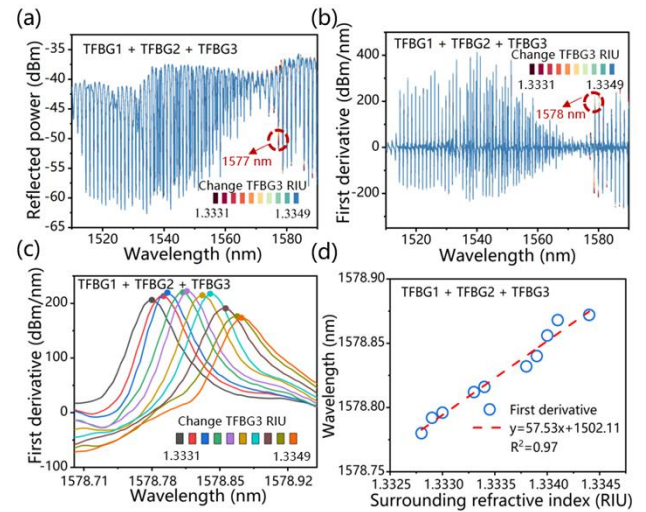


Fig. 4 (a) Evolution of the two-pass transmission amplitude spectrum as a function of the TFBG3 surrounding RI value; (b) evolution of the derivative of the two-pass transmission amplitude spectrum as a function of the TFBG3 surrounding RI value; (c) zoom around the derivative of the two-pass transmission amplitude spectrum; (d) linear fit of the derivative of the two-pass transmission amplitude spectrum.

Conclusions This work demonstrates a quasi-distributed refractive index sensing strategy based on cascaded tilted fiber Bragg gratings (TFBGs) interrogated within a single spectral channel. By combining tailored grating parameters with first-order derivative spectrum analysis, overlapping cladding-mode features can be clearly resolved. The approach enables reliable multipoint sensing with sensitivities around 53–58 nm/RIU, high linearity, and negligible cross-talk, offering a compact and scalable platform for chemical and biological sensing applications.